Gene Therapy (2016) 23, 272–282

www.nature.com/gt

OPEN

ORIGINAL ARTICLE

Healthy and diseased corticospinal motor neurons are selectively transduced upon direct AAV2-2 injection into the motor cortex

JH Jara[1], MJ Stanford[1], Y Zhu[2], M Tu[1], WW Hauswirth[3], MC Bohn[4], SH DeVries[2] and PH Özdinler[1,5,6]

Direct gene delivery to the neurons of interest, without affecting other neuron populations in the cerebral cortex, represent a challenge owing to the heterogeneity and cellular complexity of the brain. Genetic modulation of corticospinal motor neurons (CSMN) is required for developing effective and long-term treatment strategies for motor neuron diseases, in which voluntary movement is impaired. Adeno-associated viruses (AAV) have been widely used for neuronal transduction studies owing to long-term and stable gene expression as well as low immunoreactivity in humans. Here we report that AAV2-2 transduces CSMN with high efficiency upon direct cortex injection and that transduction efficiencies are similar during presymptomatic and symptomatic stages in hSOD1^{G93A} transgenic amyotrophic lateral sclerosis (ALS) mice. Our findings reveal that choice of promoter improves selectivity as AAV2-2 chicken β-actin promoter injection results in about 70% CSMN transduction, the highest percentage reported to date. CSMN transduction in both wild-type and transgenic ALS mice allows detailed analysis of single axon fibers within the corticospinal tract in both cervical and lumbar spinal cord and reveals circuitry defects, which mainly occur between CSMN and spinal motor neurons in hSOD1^{G93A} transgenic ALS mice. Our findings set the stage for CSMN gene therapy in ALS and related motor neuron diseases.

Gene Therapy (2016) **23,** 272–282; doi:10.1038/gt.2015.112

INTRODUCTION

Corticospinal motor neurons (CSMN) are highly specialized long-distance projection neurons, and they are an important component of the motor neuron circuitry.[1,2] Their ability to receive, integrate, translate and transmit information toward spinal cord targets gives them a unique role as the 'spokesperson' of the cerebral cortex.[3] CSMN are essential for the initiation and modulation of voluntary movement that requires cortical input.[4] Execution of voluntary movement, however, involves spinal motor neurons (SMN). Therefore, proper connection and communication between the brain and the spinal cord is paramount. Even though the spinal component of the circuitry is better understood for the health and stability of motor function,[5] the knowledge on the cortical component, especially CSMN, is beginning to emerge.[6–8]

CSMN are not only critically important for the proper function of voluntary movement, but they are also clinically relevant both for motor neuron diseases and in the context of injury. CSMN degenerate together with SMN in amyotrophic lateral sclerosis (ALS), and their death is a hallmark of primary lateral sclerosis and hereditary spastic paraplegia.[9,10] Recent findings also reveal that underlying mechanisms responsible for CSMN degeneration in hereditary spastic paraplegia show striking similarities with Parkinson's and Alzheimer's disease.[11] In addition, patients develop long-term paralysis after spinal cord injury owing to progressive CSMN loss and the disconnect between the brain and the spinal cord.[2,12,13] Thus improvement of CSMN health has significant clinical implications.

Understanding the intrinsic and extrinsic factors that contribute to CSMN vulnerability and progressive degeneration represents a fundamental challenge. However, newly developed technologies and availability of novel reporter lines allow for access, labeling, isolation and visualization of CSMN at different stages of their development and during disease progression.[3,14–16] These will facilitate a better understanding of the mechanisms that are responsible for CSMN vulnerability and will call for approaches that enable specific modulation of CSMN gene expression. Thus, in the near future, we will need to deliver the genes of interest to the vulnerable neurons without inducing confounding variables in other neurons and circuitries.

Building effective and long-term treatment strategies requires genetic modulations that are stable and long lasting. Adeno-associated virus (AAV) offers several significant advantages when compared with other gene delivery systems. For example, AAV serotypes transduce different cells and neurons, do not provoke toxicity in humans, provide long-term expression, there is a wide selection of available promoters and there are continuous improvements in vector capsid engineering.[17–20] More relevant to this study, AAV-mediated retrograde transduction approaches selectively transduce CSMN within the complex and heterogeneous structure of the motor cortex, without affecting other

[1]Davee Department of Neurology and Clinical Neurological Sciences, Northwestern University, Feinberg School of Medicine, Chicago, IL, USA; [2]Department of Ophthalmology and Physiology, University of Florida, Gainesville, FL, USA; [3]Department of Ophthalmology, University of Florida, Gainesville, FL, USA; [4]Neurobiology Program, Department of Pediatrics, Ann and Robert H. Lurie Children's Hospital of Chicago Research Center Northwestern University, Feinberg School of Medicine, Chicago, IL, USA; [5]Robert H. Lurie Cancer Center, Northwestern University, Chicago, IL, USA and [6]Cognitive Neurology and Alzheimer's Disease Center, Northwestern University, Chicago, IL, USA. Correspondence: Dr PH Özdinler, Davee Department of Neurology and Clinical Neurological Sciences, Northwestern University, Feinberg School of Medicine, 303 E. Chicago Avenue, Chicago, IL 60611, USA.
E-mail: ozdinler@northwestern.edu
Received 7 April 2015; revised 1 November 2015; accepted 21 December 2015; accepted article preview online 24 December 2015; advance online publication, 21 January 2016

neurons or cell types.[15] This selective transduction revealed early apical dendrite degeneration as an important mechanism contributing to CSMN degeneration and also suggested further utilization of AAV to modulate CSMN gene expression.[3,15] These unique properties make AAV one of the best candidates for gene transfer and/or replacement studies in CSMN.

Retrograde transduction of CSMN is not feasible for clinical interventions; however, direct cortex injection of AAV is proven to be more suitable for clinical studies.[19] Therefore, we investigated the possibility of modulating CSMN gene expression upon direct AAV injection into the motor cortex. Our results reveal that highly selective transduction of both healthy and diseased CSMN is possible upon direct injection of AAV2-2 containing chicken β-actin (CBA) promoter into the motor cortex and that the choice of promoter has an important role in specificity. This study not only sets the stage for selective CSMN transduction in preclinical disease models of ALS but also enables visualization and assessment of CSMN axons and their interaction with spinal cord targets. Therefore, our findings are relevant for CSMN gene therapy in ALS, and other neurodegenerative disease, in which voluntary movement is impaired.

RESULTS

AAV serotypes that encode different capsid proteins display varied transduction efficiencies toward distinct types of cells and neurons.[21] In an effort to modulate gene expression selectively in one neuron population, it is important to determine whether any AAV serotype has preferential tropism toward the neurons of interest. Initially, seven different AAV serotypes, AAV2-1, AAV2-2, AAV2-5, AAV2-6, AAV2-7, AAV2-8 and AAV2-9, expressing enhanced green fluorescent protein (eGFP) under the control of the cytomegalovirus (CMV) promoter were tested for their ability to transduce CSMN upon direct injection into layer V of the motor cortex in wild-type (WT) mice at P30 (Figures 1a–c). AAV2-3 and AAV2-4 were not included owing to their negligible levels of neuronal transduction both in the sensory motor cortex[22] and red nucleus.[23] Single-time injections (stereotaxic coordinates = +0.5 mm anterior–posterior; 1.5 mm mediolateral; 64 nl per injection, 10 injections per motor cortex, 1.2×10^9 transducing units)[24] were aimed for layer V of the motor cortex, and tissue was collected at P60. To assess whether AAV injections were within the motor cortex, CSMN retrograde labeling was performed (Figures 1b and c). Cellular transduction was mainly within layer V of the motor cortex, with similar spread of eGFP expression in all serotypes tested (Figure 1d; Supplementary Figure S1), and CSMN identity was confirmed by the presence of red fluorescent microspheres (Figure 1e).[15]

The location of neurons and their projection fields suggest their identity.[8] We first evaluated the presence of eGFP+ cells in layer V of the motor cortex (Figure 1f). AAV serotypes showed a diverse and broad tropism to many different neurons and cell types (Figure 1f). eGFP expression was detected in pyramidal neurons of different sizes, small cells/neurons with several small thin protrusions and cells with astrocyte morphology in all serotypes, at varying degrees (Figure 1f). Presence of eGFP+ axon bundles in striatum (Figure 1g) and corticospinal tract (CST; Figure 1i) suggested transduction of subcerebral projection neurons, including CSMN. Detection of eGFP+ axons in the corpus callosum was an indicator of callosal projection neuron (CPN) transduction (Figure 1h). Among all the serotypes tested, AAV2-2 resulted in transduction of large pyramidal neurons in layer V of the motor cortex with numerous axon fibers in the striatum (Figure 1g) and axons within the CST (Figure 1i). This suggested that AAV2-2 had a higher tropism for subcerebral projection neurons, including CSMN (Figure 1i).

Co-immunolabeling of eGFP with neuronal marker NeuN revealed that almost all AAV serotypes were efficient at neuronal transduction (Figure 2a). However, comparison of neuronal transduction by AAV2-2 and all other serotypes tested (one-way analysis of variance (ANOVA) followed by Tukey's multiple comparison test) revealed a statistically higher transduction efficiency by AAV2-2 (76 ± 1%; $n = 656$), whereas other serotypes displayed about 50% transduction efficiency: AAV2-1 (51 ± 2%, $n = 280$, adjusted P-value = 0.008), AAV2-5 (46 ± 5%, $n = 220$, adjusted P-value = 0.0016), AAV2-6 (55 ± 1%, $n = 287$, adjusted P-value = 0.0269), AAV2-7 (50 ± 2%, $n = 113$, adjusted P-value = 0.005), AAV2-8 (45 ± 4%, $n = 206$, adjusted P-value = 0.001), and AAV2-9 (49 ± 7%, $n = 286$, adjusted P-value = 0.0031) (Figure 2c).

As the overarching goal is to develop approaches to achieve selective gene expression in CSMN, we investigated whether other projection neurons that are closely related to CSMN and are located in the layer V of the motor cortex, such as CPN, are also transduced. Co-immunolabeling of eGFP with CPN marker SATB2 revealed no statistical significances in the ability of the tested serotypes to transduce CPN (AAV2-1: 14 ± 2%, $n = 88$; AAV2-2: 23%, $n = 218$; AAV2-5: 19 ± 4%, $n = 152$; AAV2-8: 19 ± 1%, $n = 179$ and AAV2-9: 15 ± 1%, $n = 75$; one-way ANOVA followed by Tukey's multiple comparison test; Supplementary Figure S2). This was in agreement with low levels of eGFP+ axon fibers observed in the corpus callosum (Figure 1h). We next investigated whether any of the AAV serotypes display effective CSMN transduction (Figure 2b). In striking contrast to the low levels of CPN transduction achieved by AAV2-2, its capacity to transduce CSMN (44 ± 5%, $n = 375$) was statistically significant when compared with other serotypes (one-way ANOVA followed by Tukey's multiple comparison test). Only about 20–30% of the cells transduced by AAV2-1 (19 ± 1%, $n = 163$, adjusted P-value = 0.0003), AAV2-5 (24 ± 2%; $n = 133$, adjusted P-value = 0.002), AAV2-6 (25 ± 3%, $n = 174$, adjusted P-value = 0.0033), AAV2-7 (29 ± 1%; $n = 184$, adjusted P-value = 0.0273), AAV2-8 (29 ± 1%; $n = 179$, adjusted P-value = 0.0247), and AAV2-9 (29 ± 3%; $n = 190$, adjusted P-value = 0.0255) were CSMN (Ctip2+; Figure 2d).

Quantitative analysis of astrocyte transduction (using co-immunolabeling with a marker for astrocytes, glial fibrillary acidic protein (GFAP)) revealed low levels of transduction (AAV2-1: 21 ± 11%, $n = 163$; AAV2-2: 4 ± 3%, $n = 173$; AAV2-5: 1%, $n = 162$; AAV2-6: 1%, $n = 138$; AAV2-7: 4 ± 3%, $n = 124$; AAV2-8: 12 ± 7%, $n = 181$ and AAV2-9: 21 ± 2%, $n = 269$; one-way ANOVA followed by Tukey's multiple comparison test). Similarly, limited microglia transduction (using co-immunolabeling with a marker for microglia, Iba1) revealed no statistical differences (AAV2-1: 1%, $n = 161$; AAV2-2: 2%, $n = 117$; AAV2-5: 1%, $n = 165$; AAV2-6: 1%, $n = 106$; AAV2-7: 3 ± 2%, $n = 143$; AAV2-8: 3 ± 2%, $n = 140$ and AAV2-9: 5 ± 4%, $n = 113$; one-way ANOVA followed by Tukey's multiple comparison test). This suggests that none of the AAV serotypes tested were strong enough to target astrocytes or microglia in the motor cortex (Figures 2e and f; Supplementary Figure S3).

Our results show that AAV2-2 displays significant tropism for CSMN in comparison to all other serotypes tested (Figure 2). In an effort to improve CSMN transduction, we tested whether modifying promoter and viral capsid, the two important components that modulate specificity, would have a role in CSMN transduction. We chose to use eGFP expression under the CBA promoter in addition to AAV2-2 capsid proteins with site-directed mutagenesis replacing tyrosine with phenolalanine (Y-F). CMV enhancer attached to CBA produces a hybrid promoter (CBA) (Figure 3a), which has been previously used to enhance neuronal transduction in the central nervous system.[21,25,26] Quadruple (Y-F; 272, 444, 500, 730) or sextuple (Y-F; 252, 272, 444, 500, 704, 730) substitutions in the capsid (Figure 3a)[27] increase transduction efficiency in retinal ganglion cells by making the virus less susceptible to ubiquitination and degradation.[27]

Direct cortex injections of AAV2-2 with engineered capsid expressing eGFP under the CBA promoter were performed at P30, and data is analyzed at P60 (Figure 3b). Driving eGFP expression under the CBA promoter significantly improved CSMN

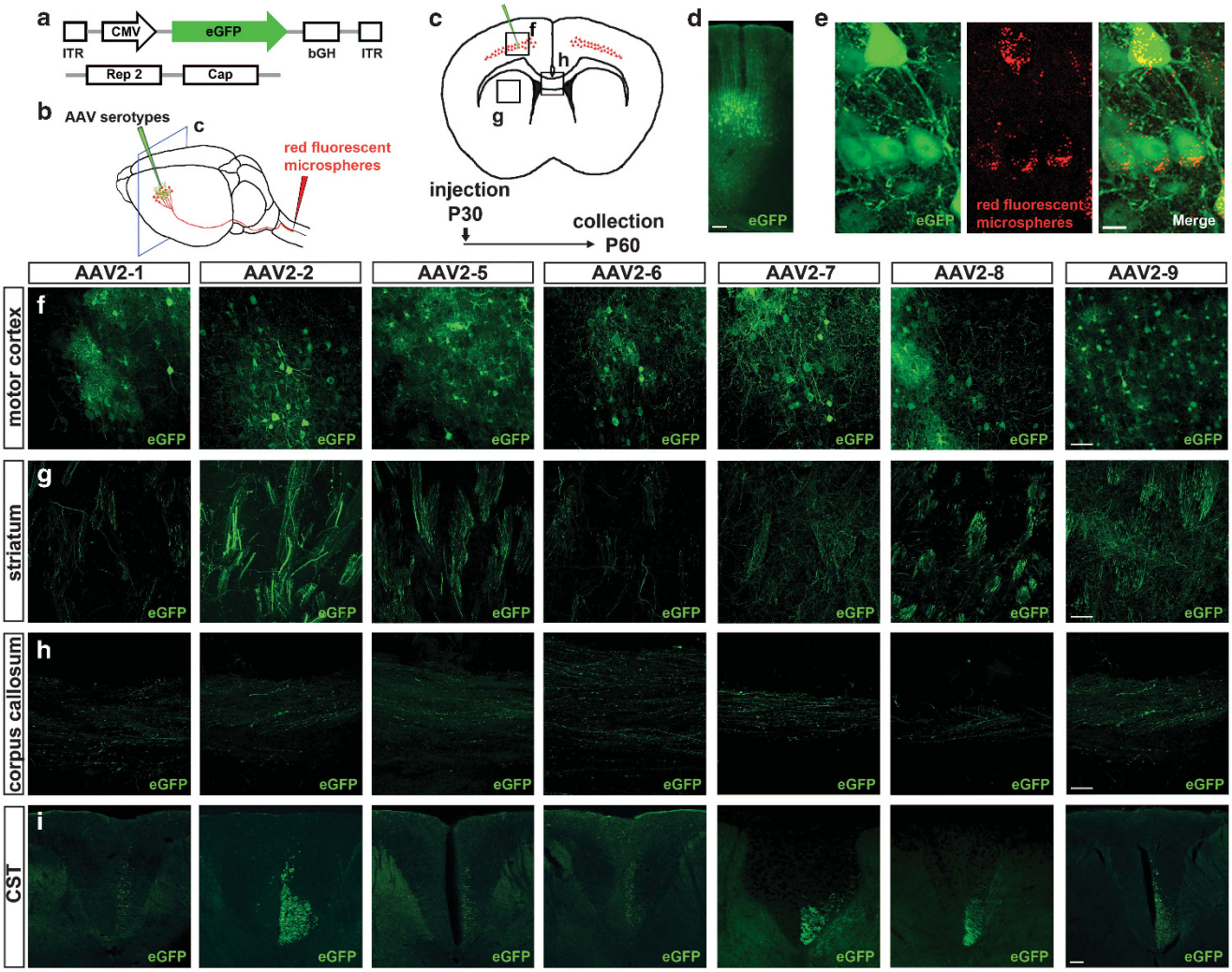

Figure 1. AAV serotypes show diverse transduction patterns in the motor cortex. (**a**) Schematic representation of an AAV *cis*-shuttle plasmid expressing eGFP under CMV promoter and *trans*-plasmid encoding for AAV2 *rep* proteins and capsids. (**b**) Experimental approach showing direct injection of different AAV serotypes and simultaneous injection of red fluorescent microspheres into the CST that lies within the dorsal funiculus of the spinal cord. All injections were performed at P30, and the tissue was collected at P60. (**c**) Schematic representation of the coronal section of the brain. The red dots represent location of CSMN, and the green arrow depicts the location of AAV injection. Boxed areas, which represent the motor cortex (**f**), striatum (**g**) and the corpus callosum (**h**), are imaged below for each serotype tested. (**d**) Representative section showing AAV2-2 injection site in the motor cortex. (**e**) Representative images of AAV2-2-transduced neurons that are also retrogradely labeled with red fluorescent microspheres, confirming that the site of injection has been the motor cortex. (**f**) Representative images of cells transduced with AAV2-1, AAV2-2, AAV2-5, AAV2-6, AAV2-7, AAV2-8 and AAV2-9 in the motor cortex. (**g**, **h**) Representative images of eGFP+ axon bundles located at the striatum (**g**) and at the corpus callosum (**h**). (**i**) Representative images of dorsal funiculus with eGFP+ axons in the CST of the cervical spinal cord. Scale bars: 100 μm (**d**), 10 μm (**e**), 50 μm (**g**–**i**).

transduction (AAV2-2 CBA, 65 ± 3% versus AAV2-2 CMV, 44 ± 5%, Figure 2d); adjusted *P*-value = 0.0191, one-way ANOVA followed by Tukey's multiple comparison test; Figures 3b–e), whereas quadruple mutations (AAV2-2 CBA 4×) in the capsid proteins did not (50 ± 3%), and sextuple mutations (AAV2-2 CBA 6×) resulted in reduction of transduction capacity (40 ± 3% adjusted *P*-value = 0.0084, one-way ANOVA followed by Tukey's multiple comparison test; Figures 3c and e).

Building effective treatment strategies to diseases require transduction of vulnerable and degenerating neurons effectively when disease is manifested. Thus we next performed cortical injections in WT and hSOD1^{G93A} transgenic ALS mice to determine whether AAV2-2 CBA transduces vulnerable neurons early in the disease (P30; presymptomatic) and when the symptoms are observed (P60) to investigate the percentage of CSMN transduced at P60 and P90, respectively (Figure 4a, Supplementary Figure S4). We find that CSMN transduction is comparable between time points and genotype (66 ± 3% for WT and 63 ± 3% for hSOD1^{G93A} mice at P60; and 64 ± 1% for WT and 64 ± 2% for hSOD1^{G93A} CSMN at P90; one-way ANOVA followed by Tukey's multiple comparison test; Figures 4b–d; Supplementary Figures S4a and b). In a subset of experiments, we tested the potential ability of AAV2-2 CBA 4x to improve transduction of diseased CSMN (Supplementary Figure S5a). We find no statistical differences in the transduction efficiency of CSMN at P60 (50 ± 3%, WT CSMN; 44 ± 10%; hSOD1^{G93A} CSMN; one-way ANOVA followed by Tukey's multiple comparison test) or at P90 (50 ± 2%, WT CSMN; 46 ± 1%; hSOD1^{G93A} CSMN; one-way ANOVA followed by Tukey's multiple comparison test; Supplementary Figures S4c and d and S5b). Upon AAV2-2 CBA injection, CPN transduction efficiency was low and comparable in both WT and hSOD1^{G93A} mice at both time points (17 ± 2% WT CPN, 17 ± 4% hSOD1^{G93A} CPN at P60; 21 ± 4% WT CPN, 20 ± 1% hSOD1^{G93A} CPN at P90; one-way ANOVA followed by Tukey's

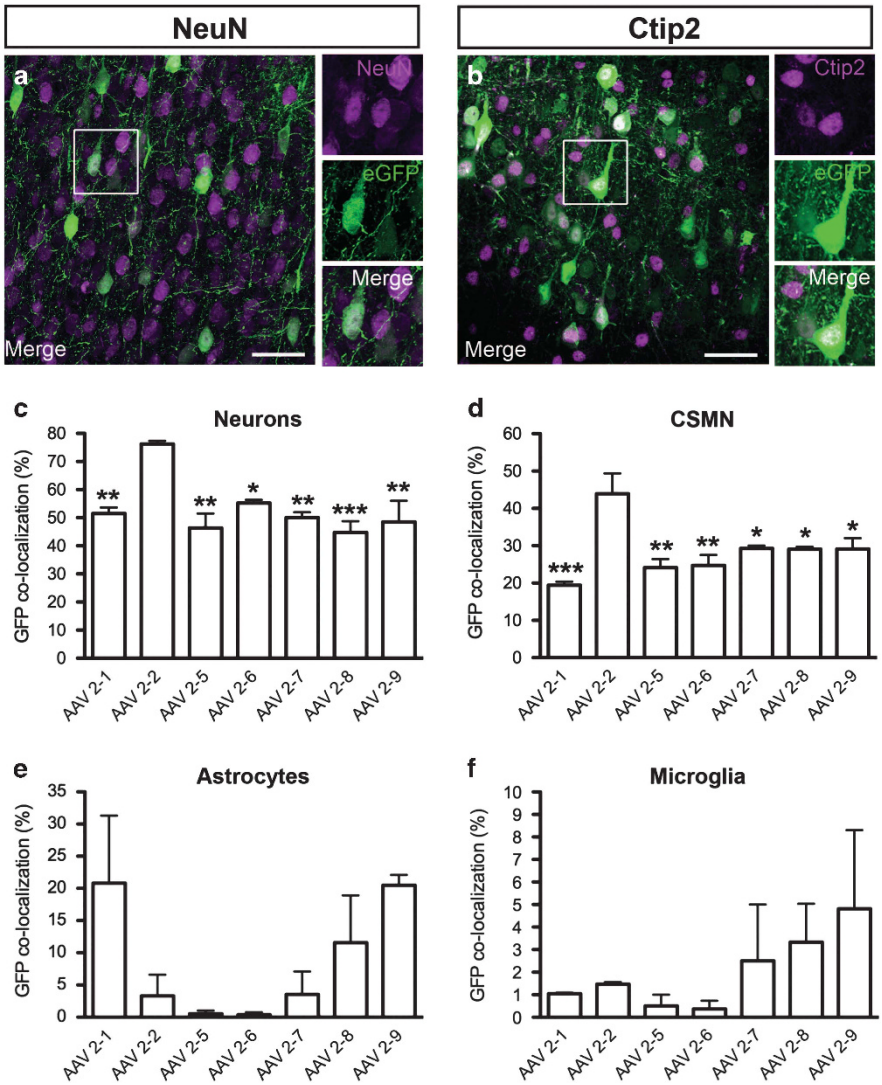

Figure 2. AAV2-2 transduces large projection neurons, mainly CSMN in the motor cortex. Co-immunolabeling with eGFP and cell-type-specific markers reveals transduction efficiencies of neurons (**a**) and CSMN (**b**) in the motor cortex. (**a**) A representative image of AAV2-2 eGFP+-transduced cells expressing NeuN. Boxed areas in representative images are enlarged to the right. (**b**) A representative image of AAV2-2 eGFP+-transduced cells expressing Ctip2. (**c**–**f**) Bar graphs represent mean percentage ± s.e.m. of neurons (eGFP+ cells, expressing neuronal marker NeuN) (**c**), CSMN (eGFP+ cells, expressing Ctip2) (**d**), astrocytes (eGFP+ cells, expressing GFAP) (**e**) and microglia (eGFP+ cells, expressing Iba1) (**f**). One-way ANOVA and Tukey's multiple comparison test, AAV2-2 versus all other serotypes. $*P < 0.05$, $**P < 0.01$, $***P < 0.001$. Scale bars 10 μm (**b**), 50 μm (**d**, **e**).

multiple comparison test, Figure 4b). Likewise, AAV2-2 CBA 4× injection resulted in similar levels of CPN transduction (17 ± 2% WT CPN, 18 ± 2% hSOD1^{G93A} CPN at P60; 18 ± 2% WT CPN, 20 ± 2% hSOD1^{G93A} CPN at P90; one-way ANOVA followed by Tukey's multiple comparison test; Supplementary Figures S5a–c). These results suggest that the choice of promoter is more effective than the mutations in the capsid protein to improve CSMN transduction and that both WT and diseased CSMN display similar transduction efficiencies at two different disease stages.

AAV2-2 CBA results in effective CSMN transduction and CST axons extending through the dorsal funiculus as well as the branching of the CST innervating both cervical and lumbar sections of the spinal cord become visible (Figure 1j). This enables investigation of CSMN connectivity in the spinal cord. We first measured the volume and length of eGFP+ CST axons fibers in both WT and hSOD1^{G93A} cervical and lumbar spinal cord at P90 using Fiji's Simple Neurite Tracer plugin (Figure 5).[28] The average cross-sectional area was then obtained by dividing the relative volume for each axon segment by its respective length. There were no statistical differences between the cross-sectional areas of CST in either the cervical (WT: 1.3 ± 0.1 μm^2; hSOD1^{G93A}: 1 ± 0.2 μm^2) or lumbar (WT: 0.8 ± 0.1 μm^2; hSOD1^{G93A}: 0.7 ± 0.1 μm^2) spinal cords of WT and hSOD1^{G93A} mice (normality D'Agostinos and Pearson test, two-tailed unpaired *t*-test, Figures 5a–c and e). However, close examination of CST branches projecting to the ventral horn of spinal cord revealed that the axonal projections in the lumbar spinal cord were significantly impaired (WT: 0.8 μm^2; hSOD1^{G93A}: 0.5 μm^2, normality D'Agostinos and Pearson test, two-tailed unpaired *t*-test, $P = 0.0356$), whereas projections at the cervical level were comparable (WT: 0.7 μm^2; hSOD1^{G93A}: 0.8 μm^2; normality D'Agostinos and Pearson test, two-tailed unpaired *t*-test, NS).

To investigate potential CSMN–SMN and CSMN–interneuron interaction defects in the hSOD1^{G93A} mice at P90, we performed eGFP/choline acetyltransferase (ChAT) (WT: $n = 4$; hSOD1^{G93A}: $n = 8$) and eGFP/calretinin+calbindin (WT: $n = 4$; hSOD1^{G93A}: $n = 6$) immunocytochemistry in both cervical and lumbar spinal cord (Figure 6). When the CST and the neuron have a connection, we expect to see an eGFP+ axon fiber either in contact (Figure 6e)

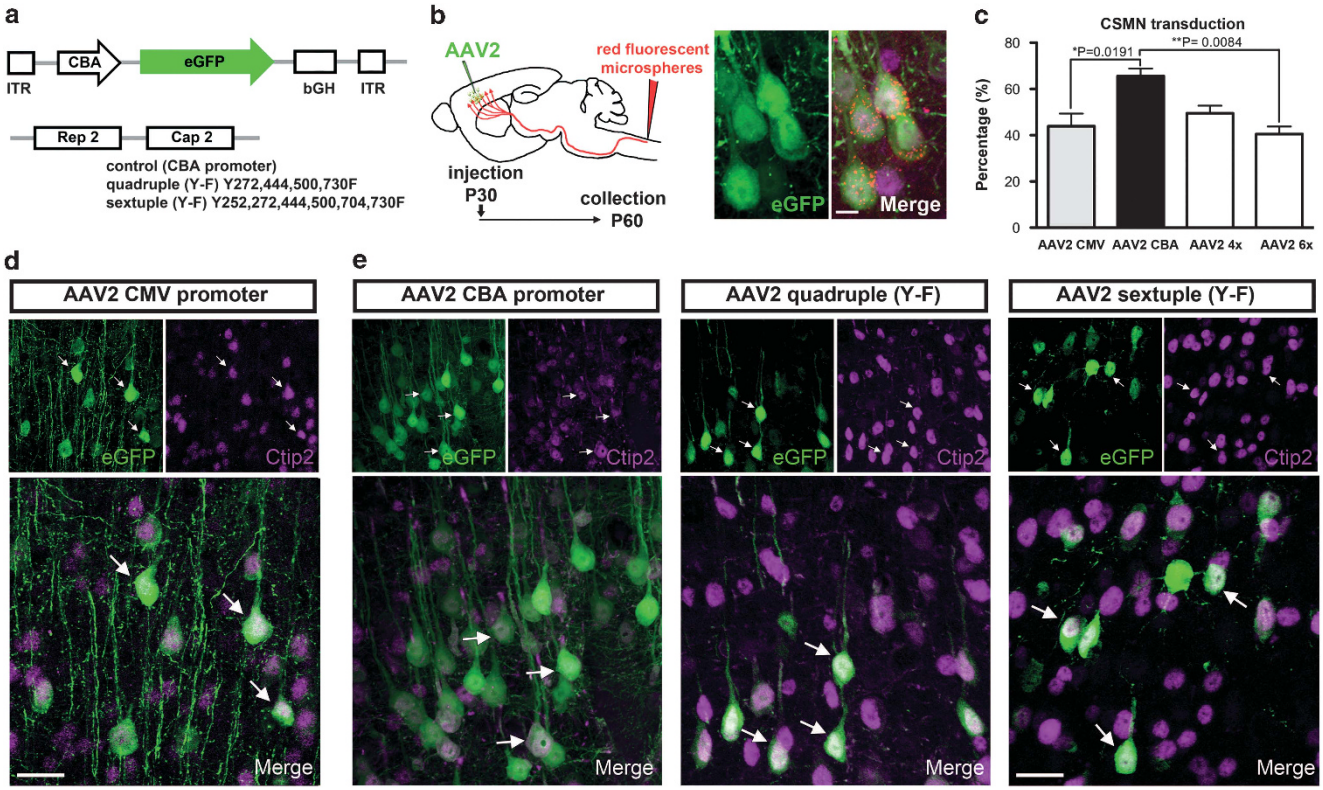

Figure 3. AAV2-2 containing CBA promoter has high tropism for CSMN. (**a**) Schematic representation of an AAV *cis*-shuttle plasmid expressing eGFP under the CBA promoter and *trans*-plasmid encoding for AAV2-2 *rep* proteins and capsid. Modified capsids used in this study contained four (AAV quadruple Y-F) and six (AAV sextuple Y-F) tyrosine to phenylalanine point mutations. (**b**) Experimental approach showing direct injection of AAV2-2 and simultaneous injection of red fluorescent microspheres into the CST. All injections were performed at P30, and the tissue was collected at P60. Representative image of AAV2-2-transduced neurons that are also retrogradely labeled with red fluorescent microspheres (orange-red punctate) and immunostained for Ctip2 (purple) confirming their CSMN identity. (**c**) Bar graphs represent mean percentage ±s.e.m. of CSMN (eGFP+ cells, expressing Ctip2) transduction with different AAV2-2. (**d**) Representative images of neurons transduced with AAV2-2 encoding eGFP under the CMV promoter. Arrows indicate eGFP+ neurons expressing Ctip2. (**e**) Representative images of neurons transduced with AAV2-2 encoding eGFP under the CBA promoter (left), AAV2-2 encoding eGFP under the CBA promoter containing four (AAV2-2 quadruple Y-F) tyrosine to phenylalanine point mutations (middle panel) and AAV2-2 encoding eGFP under the CBA promoter containing six (AAV2-2 sextuple Y-F) tyrosine to phenylalanine point mutations (right panel). Arrows indicate eGFP+ neurons expressing Ctip2. One-way ANOVA and Tukey's multiple comparison test. $*P < 0.05$, $**P < 0.01$. Scale bar = 20 μm.

or in close proximity to the neuron. Our results indicated that about 75% of WT SMN (cervical: WT, 75 ± 2%; lumbar: WT, 68 ± 2%; Figures 6a and c) and 60% of interneurons (cervical: WT, 61 ± 2%; lumbar: WT, 54 ± 3%; Figures 6a and d) are in close proximity (5–10 μm) to eGFP+ axons in the cervical and lumbar sections of the spinal cord. However, in the hSOD1^{G93A} mice the percentages of SMN that either have direct contact or are located in close proximity to eGFP+ axons were significantly reduced (cervical: hSOD1^{G93A}, 45 ± 5%, $P = 0.0040$, Mann–Whitney test; lumbar: hSOD1^{G93A}, 21 ± 2%, $P = 0.0040$, Mann–Whitney test; Figures 6b and c). CSMN–interneuron interactions were also impaired even though to a lesser degree (cervical: hSOD1^{G93A} 48 ± 4%, $P = 0.0095$, Mann–Whitney test; lumbar: hSOD1^{G93A} 42 ± 3%, $P = 0.0238$, Mann–Whitney test; Figures 6b and d). Co-immunolabeling studies with synaptophysin (presynaptic marker) and PSD-95 (postsynaptic marker) further confirm the existence of CSMN–SMN interaction and the presence of excitatory synapse (Figure 6e).

Our findings reveal some important aspects of CSMN transduction upon direct cortex injection. We find that: (1) AAV2-2 serotype shows relatively higher tropism to CSMN in the motor cortex; (2) CSMN, but not CPN, transduction efficiency increases when CBA promoter is used; (3) upon direct cortex injection of AAV2-2 CBA, about 70% of CSMN and 20% CPN are transduced; (4) transduction efficiencies of healthy and vulnerable CSMN are similar and the rate of transduction is comparable between presymptomatic (P30) and symptomatic (P60) stages; (5) effective CSMN transduction allows visualization of CST axon fibers and their projections into ventral horn of the spinal cord; and (6) the most severely affected connection is between CSMN and SMN in hSOD1^{G93A} transgenic ALS mice.

DISCUSSION

CSMN have a unique ability to collect, integrate, translate and transmit cortical input toward spinal cord targets. For many years, their degeneration has been considered secondary to SMN death in ALS and has been mostly ignored. However, recent findings reveal that their vulnerability is an early event in the disease and that they are critical contributors to ALS disease pathology,[7,29,30] emphasizing the need to modulate their gene expression for building effective treatment strategies in the future.

The low toxicity and ability to sustain long-term gene expression makes AAV an ideal tool to deliver the genes of interest into cells and neurons, and therefore they are commonly used in clinical settings.[18,19,21] Even though AAV has not yet been used in clinical trials for ALS, numerous preclinical studies using mouse and rat models of ALS have demonstrated feasibility upon systemic and local applications. Initially, SMN were targeted by muscle injections of AAV, allowing retrograde transduction of SMN subsets based on their projection field.[31–33]

Retrograde transduction of SMN with AAV2-IGF-1 (insulin-like growth factor 1) increased survival and motor function in hSOD1^{G93A} transgenic ALS mice.[34] In addition, transducing choroid plexus cells with AAV-4 expressing IGF-1 or vascular endothelial growth factor resulted in continuous production and homogeneous distribution of growth factors in the cerebrospinal fluid, resulting in the moderate extension of survival in hSOD1^{G93A} mice with delayed motor decline.[35] More interestingly, intravenous administration of AAV2-6 expressing short hairpin RNA (shRNA) targeting mutant SOD1 was able to transduce SMN at all levels in the spinal cord but did not change disease progression.[36] More recently, a study using AAV2-9 has demonstrated a unique ability to cross the blood–brain barrier to predominately transduce astrocytes in the adult mouse brain and spinal cord.[37] This approach slowed disease onset and progression in the ALS mouse model after single injection of AAV2-9 encoding an shRNA against SOD1.[38]

A recent study targeted the motor cortex in the hSOD1^{G93A} rat model and significantly reduced the levels of SOD1^{G93A} expression by injecting AAV2-9-SOD1-shRNA. This showed remarkable improvement and increased SMN survival, as well as an extension in lifespan,[30] suggesting that cortical interventions could provide a significant therapeutic benefit. Previously, Foust *et al*.[39] used AAV-mediated anterograde transduction strategy to transduce cortical neurons. This was a rather novel approach at the time. With this idea, AAV5-CBA-GDNF was injected directly into the primary sensorimotor cortex resulting in the detection of GDNF in the cortex, striatum and thalamus.[39] Moreover, CSMN transduction efficiency toward seven different AAV serotypes and lentivirus was also tested.[22] Hutson *et al*.[22] showed that AAV2-1 and AAV2-5 diffused to a larger area within the sensorimotor cortex and thus transduce higher number of neurons. Interestingly, they also report significantly higher levels of astrocyte transduction especially with AAV2-1. These findings suggest that the preparation and the concentration used could increase tropism for both neurons and non-neuronal cells in the sensorimotor cortex, especially in the layers V–VI. Our results are in partial agreement with these findings. For example, we observe low levels of astrocyte transduction in the presence of AAV2-1, -2, -5, -6 and -8. In addition, we report that upon AAV2-1 injection about 25% CSMN are transduced, a comparable finding of approximately 30% CSMN transduction.[22] As AAV2-1, but not AAV2-2, diffused in a larger area and the data are analyzed as total neurons,[22] it is possible that the percentage of efficiency was underscored. In addition, it is also possible that different AAV serotypes show preferential tropism in motor versus sensorimotor cortex in mice and rats.

The variations in neuronal transduction could be due to differences in the location of application, virus preparation and/or concentration.[40,41] Transduction properties of AAV serotypes in striatum, substantia nigra, globus pallidus and hippocampus were tested[21,42,43] and revealed that AAV2-1 and AAV2-5 transduce neurons more effectively than AAV2-2 upon direct midbrain, striatum and hippocampus injection.[43,44] AAV2-7, AAV2-8 and AAV2-5 transduced neurons almost exclusively in caudate-putamen, substantia nigra and hippocampus.[41] On the other hand, AAV2-9 transduced neurons more robustly in the hippocampus and cerebral cortex when compared with AAV2-8.[40] A more recent and comprehensive analysis in the auditory cortex suggested that, in addition to robust neuronal transduction, small numbers of astrocytes, microglia and oligodendrocytes are also transduced by a distinct set of AAV serotypes.[45] However, none of these studies performed detailed cellular or molecular marker expression analysis to determine the identity of the neurons transduced. AAV2-8 displayed astroglial transduction upon cesium chloride purification but a neuronal transduction when purified with iodixanol.[25] Stability and expression of GFP is also likely to be influenced by specific promoters. Of interest, differential transduction of inhibitory and excitatory neurons was achieved by applying AAV2-1 with human synapsin promoter at different concentrations.[46] Declined duration of AAV vector expression using CMV promoters have been attributed to methylation

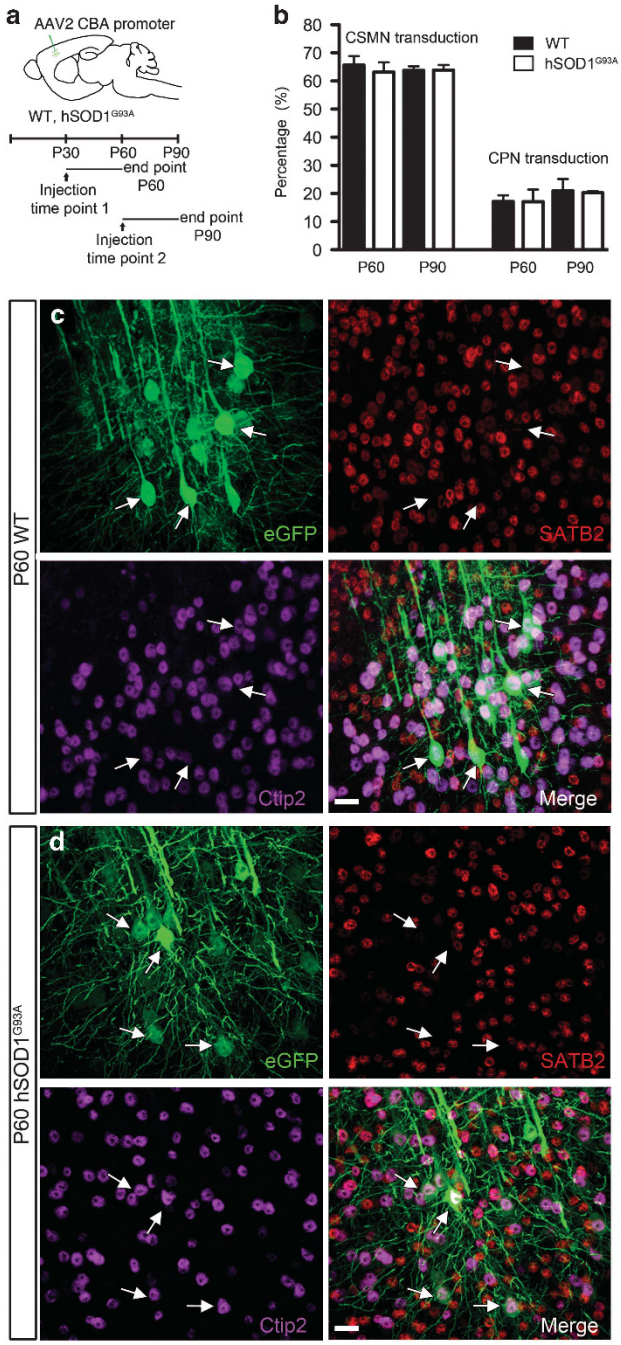

Figure 4. AAV2-2 with CBA promoter transduces both WT and diseased CSMN. (**a**) Experimental approach showing direct injection of AAV2-2 CBA. Injections were performed at P30 and P60, and the tissue was collected at P60 and P90, respectively. (**b**) Bar graphs represent mean percentage ± s.e.m. of CSMN (eGFP+ cells, expressing Ctip2) and CPN (eGFP+ cells, expressing SATB2) transduction in both WT and hSOD1^{G93A} mice at P60 and P90. (**c**) Representative images of P60 WT neurons transduced with AAV2-2 encoding eGFP under the CBA promoter. Arrows indicate eGFP+ neurons expressing Ctip2 and not SATB2. (**d**) Representative images of hSOD1^{G93A} neurons transduced with AAV2-2 encoding eGFP under the CBA promoter. Arrows indicate eGFP+ neurons expressing Ctip2 and not SATB2. No statistical differences were detected by one-way ANOVA and Tukey's multiple comparison test. Scale bar = 20 μm.

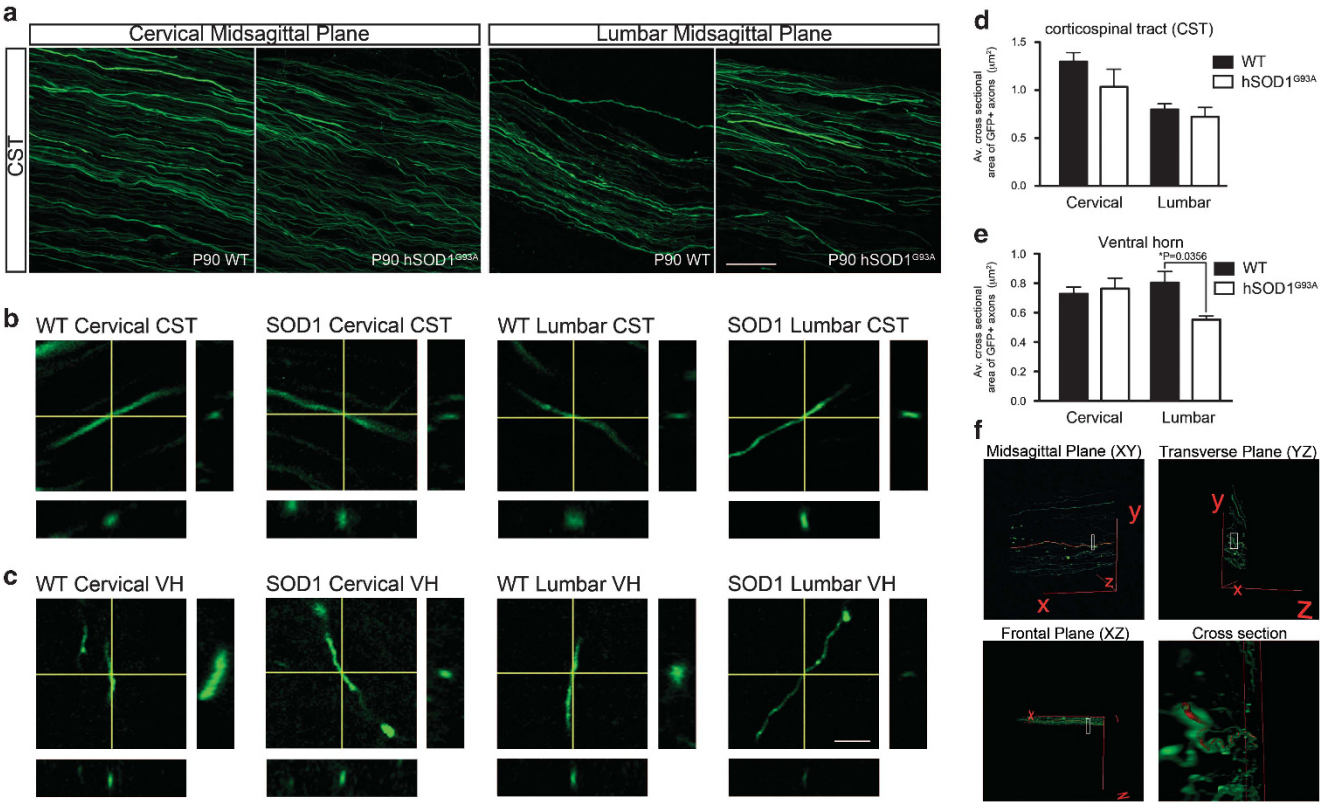

Figure 5. CST axons exhibit smaller cross-sectional area in the ventral horn of hSOD1^{G93A} mice. (**a**) Representative image of AAV2-2 CBA-transduced axons in the midsagittal plane from WT and hSOD1^{G93A} in the cervical and lumbar CST. (**b**) Representative orthogonal images of AAV2-2 CBA-transduced axons from WT and hSOD1^{G93A} in the cervical and lumbar CST (**c**) and ventral horn (VH). (**d**) Bar graph represents the mean cross-sectional area ± SEM of eGFP+ axons in the CST of WT and hSOD1^{G93A} cervical and lumbar spinal cord (μm^2). (**e**) Bar graph represents the mean cross-sectional area ± s.e.m. of eGFP+ axons in the VH of WT and hSOD1^{G93A} cervical and lumbar spinal cord (μm^2). (**f**) Representative 3D image displaying a single axon of the CST rotated in three 2d planes (XY midsagittal plane, YZ transverse plane, XZ frontal plane), with an additional image representation of the axon's cross-sectional area. D'Agostinos and Pearson normality test and two-tailed unpaired *t*-test, $^{**}P < 0.01$. Scale bar **a**, **f** = 20 μm; **b**, **c** = 5 μm.

of viral-regulatory sequences. This has led to the exploration of other promoters. For instance, CBA enhancer attached to CMV produces a hybrid promoter (CBA) that considerably reduces downregulation of GFP and results in a stronger GFP expression over time.[21,25,26] Achieving selective or improved tropism by using different promoters is an emerging theme. For example, cone cells in the pig retina were transduced more effectively when the CMV promoter was used, whereas GRK1 promoter was not successful.[47] Likewise, CMV promoter in AAV2-9 transduced cardiac tissue, while the same virus with CBA promoter transduced liver cells more effectively in mice.[48]

We think that modulation of gene expression only within a select set of neuron population, without affecting other neurons or cells in the cerebral cortex, is critically important for both visualization and assessment of their projection and target interaction. CSMN–SMN and CSMN–interneuron interactions have been an active area of research. In an effort to visualize CSMN axons, previous studies employed AAV injection into the sensorimotor cortex, which allowed visualization of CST axon fibers in the ventral horn of WT mice.[22] The timing and extent of CST degeneration in hSOD1^{G93A} mice was mainly studied by crossing CST-YFP reporter line with hSOD1^{G93A} mice. These studies revealed progressive CST degeneration between P90 and P120[29] and the presence of small varicosities and axonal fragmentation with swellings in both cervical and lumbar spinal cord mostly in the lateral dorsal funiculus.[49] None of these studies were able to bring high resolution and allow for direct assessment of CSMN–SMN and CSMN–interneuron interactions in diseased ALS transgenic mouse. Previous electrophysiological and reconstruction studies of the CST branching studies using *in vitro* slice co-cultures of rat sensorimotor cortex slices[50–52] and the investigation of CST axon fibers in YFP reporter line[2,53,54] suggested direct connections between CSMN–SMN and CSMN–interneurons. However, the extent of connectivity defects remained elusive in disease. As enhanced CSMN transduction enabled visualization of single CST axon fibers in both WT and hSOD1^{G93A} ALS mouse model, our studies revealed very precise aspects of axonal pathology and suggested that CSMN–SMN interactions were affected more than CSMN–interneuron interactions during symptomatic stages.

We previously reported retrograde transduction of CSMN upon direct injection of AAV into the CST in both WT and diseased ALS mice.[15] This approach allowed very precise CSMN transduction and revealed that spine loss and apical dendrite degeneration is an early event in ALS. These findings were supported by the recent report that shows CSMN spine loss as early as P14 in the diseased CSMN.[7] Even though CSMN can be very selectively targeted via direct injection into the CST in the mouse, owing to anatomical differences between mice and humans, this approach would not be optimal for clinical interventions. Building effective and long-term treatment strategies to motor neuron diseases may require selective or enhanced CSMN transduction together with SMN. We think that systemic application may produce global transduction but may not be particularly strong in the neurons of interest. Thus selective modulation of gene expression in vulnerable neurons without affecting other neurons,

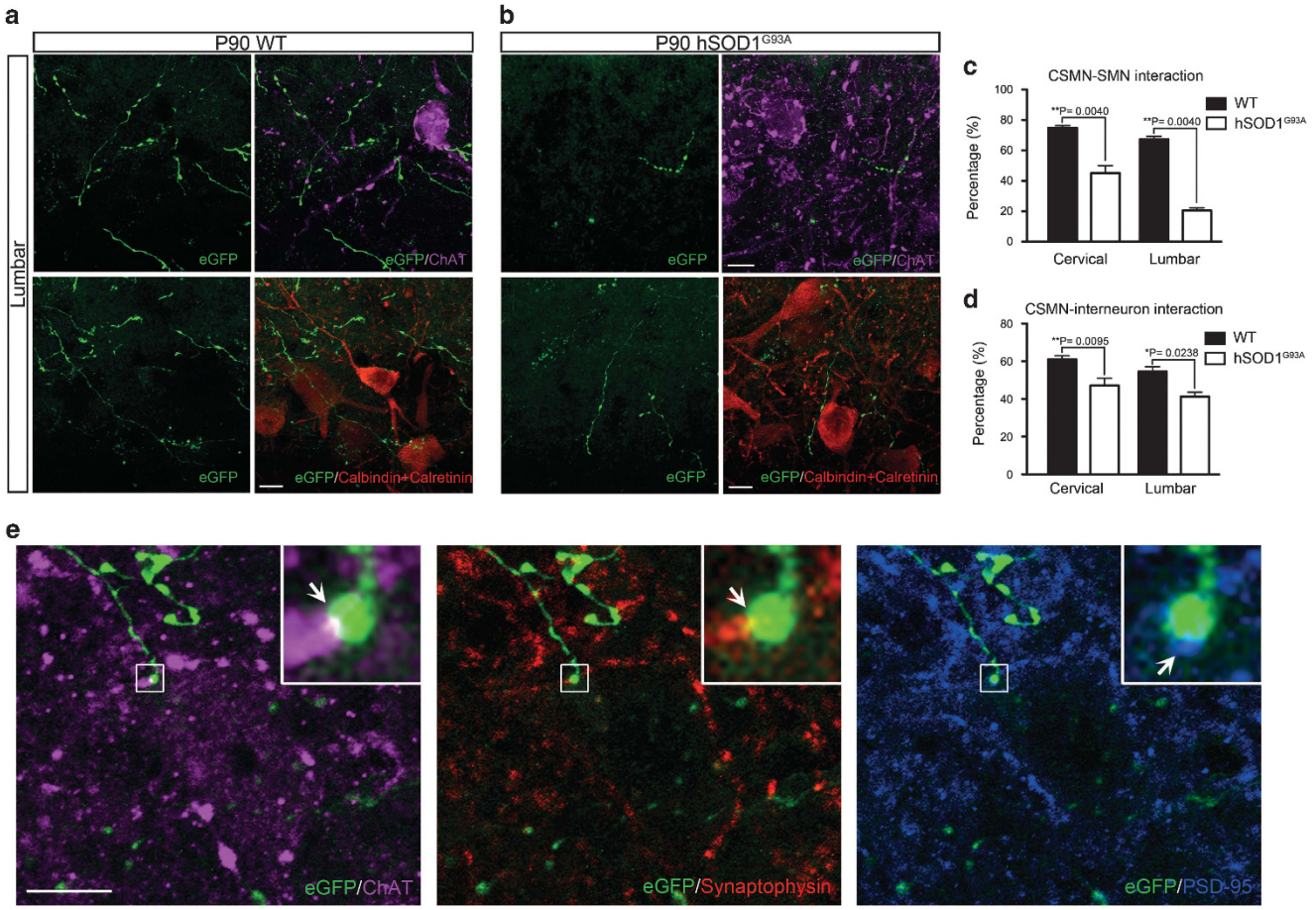

Figure 6. CSMN–SMN interaction is significantly reduced in hSOD1^{G93A} mice. (**a**) Representative image of AAV2-2 CBA-transduced lumbar axons interacting with interneurons (Calbindin+/calretinin+) and SMN (ChAT+) in WT mice. (**b**) Representative image of AAV2-2 CBA-transduced lumbar axons interacting with interneurons (Calbindin+/calretinin+) and SMN (ChAT+) in hSOD1^{G93A} mice. (**c**) Bar graph represents mean percentage ± s.e.m. of SMN interacting or in close proximity with eGFP+ CST axons in WT and hSOD1^{G93A} in the cervical and lumbar spinal cord. (**d**) Bar graph represents mean percentage ± s.e.m. of interneurons interacting or in close proximity with eGFP+ CST axons in WT and hSOD1^{G93A} in the cervical and lumbar spinal cord. (**e**) Representative image of direct synaptic contact between CST (eGFP+ axon) and SMN (ChAT+, purple). Axon colocalizes with presynaptic marker synaptophysin (red), and it is juxtapose to postsynaptic marker PSD-95 (blue). Mann–Whitney test, $*P < 0.05$, $**P < 0.01$. Scale bar = 10 μm.

cells or circuits in the cerebral cortex is paramount. Here we demonstrate improved transduction efficiency of CSMN by AAV2-2 CBA in a preclinical model, and as direct cortex injection is more tolerable and is easily accessible in patients, we anticipate the validity of this approach for future clinical trials.

MATERIALS AND METHODS

Mice used in this study are all in C57BL/6 background. hSOD1^{G93A} transgenic ALS mice overexpressing the human SOD1 G93A mutation (B6SJL-Tg(SOD1*G93A)1Gur/J) were initially obtained from Jackson Immuno Research Laboratories[55] (Bar Harbor, ME, USA) and were crossed at least six generations with mice in C57BL/6 background to bring all mice to the same background prior to experimental analysis. In this study, both females and males were used. WT, non-transgenic littermates were used as controls. Genotypes of mice were determined as described by the vendor. All animal procedures were approved by the Northwestern University Animal Care and Use Committee and conformed to the standards of the National Institutes of Health.

Adeno-associated viruses

AAV2 vectors containing CMV promoter was generated by the University of Pennsylvania Vector Core facility by triple transfection of subconfluent HEK293 cells. The plasmids used for transfections were as follows: (1) *cis*-plasmid pENN.AAV.CMV.PI.eGFP.WPRE.bGH containing and eGFP expression cassette under the CMV promoter and flanked by AAV2 inverted terminal repeats (Figure 1a), (2) *trans*-plasmids pAAV2/1, pAAV2/2, pAAV2/5, pAAV2/6, pAAV2/7, pAAV2/8 and pAAV2/9 containing the AAV *rep* gene and capsid protein genes from AAV1, 2, 5, 6, 7, 8 and 9, respectively (Figure 1a), and (3) an adenovirus helper plasmid pAdΔF6. Large-scale polyethylenimine-based triple transfections were performed, and the culture medium containing the vector particles was collected, concentrated by tangential flow filtration and purified by iodixanol gradient ultracentrifugation followed by further concentration and buffer exchange as previously described.[56]

AAV2 vectors containing the hybrid CMV enhancer/CBA promoter and eGFP were prepared from pTR-UF11 plasmid and according to previously described methods[57,58] (Figure 3a). The 1.7-kb CBA promoter is a hybrid promoter containing CMV early enhancer element (~0.4 kb), CBA promoter (~1.2 kb fragment of the promoter, the first exon and the first intron of CBA gene) and the splice acceptor of the rabbit β-globin gene (~0.1 kb). Site-directed mutagenesis of surface-exposed tyrosine residues on AAV2 VP3 provided AAV quadruple (Y-F; 272, 444, 500, 730) and AAV sextuple (Y-F; 252, 272, 444, 500, 704, 730) Y-F capsid mutant versions of AAV2-2 containing CBA promoter.[27,59]

Surgical procedures

Surgeries were performed on mice that were deeply anesthetized with isoflurane and placed into a stereotaxic platform. Micro-injections were performed using pulled-beveled glass micro-pipettes attached to a nanojector (Drummond Scientific, Broomall, PA, USA). Both CSMN labeling and transduction surgeries were performed on the same day. Surgeries

were performed at P30, and data is analyzed at P60 ($n=3$). For studies in WT and hSOD1^{G93A} mice, surgeries were performed at P30 and P60. Data is analyzed at P60 and P90 ($n=3$).

CSMN labeling

All surgeries were performed as previously described.[29] Briefly, a small laminectomy at the cervical spinal cord (C2–C3) level was performed to expose the spinal cord. CSMN were retrogradely labeled by injection of fluorescent microspheres (LumaFluor Inc., Naples, FL, USA; ~207 nl) into the CST that lies within the dorsal funiculus (df) at 0.3 mm depth.

Transduction surgeries into the motor cortex

CSMN were transduced by AAV2-1, AAV2-2, AAV2-5, AAV2-6, AAV2-7, AAV2-8 or AAV2-9 serotypes encoding eGFP under the CMV promoter. In another set of experiments, CSMN of WT and hSOD1^{G93A} mice were transduced by AAV2-2, AAV2-2 quadruple Y-F and AAV2-2 sextuple Y-F encoding eGFP under the CBA promoter. To inject the different serotypes into the motor cortex, a small unilateral craniotomy of ~5 mm^2 (coordinates = +0.5 mm anterior–posterior; 1.5 mm mediolateral) was performed into the left hemisphere using a microdrill (Fine Science Tools, Foster City, CA, USA). Ten injections of 64 nl were performed to target the primary and secondary motor cortex for a total of 640 nl containing 1.2×10^9 transducing units per mouse.

Tissue collection and immunocytochemistry

Mice were deeply anesthetized with ketamine (90 mg kg^{-1}) and xylazine (10 mg kg^{-1}) and perfused with 4% paraformaldehyde in phosphate-buffered saline (PBS). The brains were removed intact and postfixed by 4% paraformaldehyde overnight and then kept in PBS–sodium azide (0.01%) at 4 °C. Brains were sectioned coronally at 50-μm thick sections using a vibrating microtome (VT1000S, Leica Instruments, Nussloch, Germany). All antibodies used in this study were purchased from Millipore (Billerica, MA, USA) unless otherwise noted. Polyclonal anti-GFP (1:1000; Abcam, Cambridge, MA, USA; ab13970), polyclonal anti-GFP (1:1000; Invitrogen, Carlsbad, CA, USA; A11122), monoclonal anti-Ctip2 (1:500; Abcam, ab18465), monoclonal anti-GFAP (1:2000; Invitrogen, 13-0300), polyclonal anti-Iba1 (1:500; Wako, Richmond, VA, USA; 019-19741), monoclonal anti-NeuN (1:1000; MABN140), polyclonal anti-ChAT (1:200; AB144P), polyclonal anti-Calretinin (1:500; AB5054), polyclonal anti-Calbindin (1:500; AB1778), monoclonal anti-SATB2 (1:1000; Abcam, ab51502), monoclonal anti-synaptophysin (1:200; MAB368), polyclonal anti-PSD95 (1:200; Abcam, ab12093) and polyclonal anti-PSD95 (1:200 Life Technologies, Carlsbad, CA, USA; 516900) were used. The fluorescent secondary antibodies were purchased from Molecular Probes (Eugene, OR, USA) unless otherwise noted. Goat anti-chicken Alexa 488 (1:1000; A11039), goat anti-rabbit Alexa 488 (1:1000; A11008), goat anti-mouse Alexa 647 (1:1000; A21235), goat anti-rat Alexa 647 (1:1000; A21247), goat anti-rabbit Alexa 647 (1:1000; A21245), goat anti-mouse Cy3 (1:1000; Jackson ImmunoResearch Laboratories, 115-167-020), donkey anti-goat Alexa 647 (1:500; A21447), donkey anti-goat Alexa 647 (1:500; A21447), donkey anti-rabbit Alexa 555 (1:1000; A31572), donkey anti-rabbit Dylight 405 (1:200; Jackson ImmunoResearch Laboratories, 711-475-152), donkey anti-mouse Cy3 (1:200; Jackson ImmunoResearch Laboratories, 715-165-150), and donkey anti-chicken fluorescein isothiocyanate (1:1000; Jackson ImmunoResearch Laboratories, 703-095-115) were used. Immunocytochemical staining protocols were performed in free-floating brain or spinal cord sections depending on the primary antibody combination utilized for the experiment. Immunostaining protocol for GFP alone or in combination with NeuN and Iba-1 consisted of incubation with blocking solution (PBS, 0.05% bovine serum albumin, 2% fetal bovine serum, 1% Triton X-100 and 0.1% saponin) for 30 min at room temperature and overnight incubation at 4 °C with primary antibody/ies diluted in blocking solution. The next day, three washes with PBS were followed by 2 h incubation at room temperature with appropriate secondary antibody/ies diluted in blocking solution. After three washes with PBS, sections were mounted on slides and coversliped using Fluoromount G (Electron Microscopy Sciences, Hatfield, PA, USA). For GFP in combination with Ctip2 and SATB2, the above-mentioned immunostaining procedure was followed except that sections were subjected to antigen retrieval with 0.01 M sodium citrate pH = 9 for 3 h in a water bath at 80 °C previous to blocking. Immunostaining protocol for GFP/ChAT, GFP/Calbindin+Calretinin, GFP/ChAT/synaptophysin/PSD95 and GFP/Calbindin+Calretinin/synaptophysin/PSD95 consisted of three washes with PBS/0.3% Triton X-100 followed by incubation with blocking solution (PBS, 5% bovine serum albumin, 4% donkey serum, 0.3% Triton X-100) for 30 min at room temperature and overnight incubation at 4 °C with primary antibody/ies diluted in blocking solution. The next day, three washes with PBS/0.3% Triton X-100 were followed by 2-h incubation at room temperature with appropriate secondary antibody/ies diluted in blocking solution. After three washes with PBS, sections were mounted on slides and coversliped using Fluoromount G (Electron Microscopy Sciences).

Imaging

Nikon Eclipse TE2000-E fluorescence microscopes equipped with Intensilight C-HGFI (Nikon Inc., Tokyo, Japan) was used. Epifluorescence images were acquired using a Digital Sight DS-Qi1MC CCD camera (Nikon Inc.), and light images were acquired using a Ds-Fi1 camera (Nikon Inc.). Confocal images were collected using a Zeiss 510 Meta confocal microscope (Carl Zeiss Inc.).

Quantification and statistical analysis

For all statistical analysis, $n=3$ mice were used for each genotype and time point, unless otherwise noted in the Results section. For quantification of CSMN and other cell types, at least three representative sections at ×20 from the motor cortex were taken.

Percentage of transduced cells that express cell-type-specific markers were quantified ($n=3$ sections per mouse) by counting cells that express eGFP and cells that express eGFP and the selected marker (that is, GFAP (astrocyte), Iba1 (microglia), NeuN (mature neuron), Ctip2 (CSMN) and SATB2 (CPN).

Cervical and lumbar spinal cords were sagittally sectioned to reveal details of the CST and axially to help visualize connectivity of branching CST axons with SMN and interneurons. Co-presence of eGFP+ CST axons in the vicinity of interneurons (calbindin+ and/or calretinin+) and SMN (ChAT+) were quantitatively measured. Neurons that have direct contact with CST and that are in close proximity (5–10 μm) to CST fibers were quantified in both cervical and lumbar spinal cord of WT and hSOD1^{G93A} mice at P90.

Cross-sectional volumetric analysis. Confocal *z*-stacks were collected from sections using a Zeiss 510 Meta confocal microscope (Carl Zeiss Inc., Oberkochen, Germany). The resulting stacks were loaded into the open source software platform Fiji (Fiji/Image J http://imagej.nih.gov/ij/i, NIH).[60] Individual neurons were traced in a 3D pane view and a Hessian-based analysis was applied utilizing Fiji's Simple Neurite Tracer plugin as previously described to create comparable volume reconstructions.[28] Using the 'fit to volume' feature, each neuron trace was filled out using the Dijkstra's algorithm at a set intensity of 0.005 (determined by taking the average of adjusted thresholds from each axon) for the axons in the ventral horn and an adjusted threshold for the axons in the CST to obtain the relative volume and length of each traced neuron segment. Individual traces ranged from 4 to 10 μm in length. The average cross-sectional area was then obtained by dividing the relative volume for each axon segment by its respective length. The analysis was performed in both cervical and lumbar spinal cords at P90. For axons in the ventral horn, 2 sections were analyzed per mouse and approximately 10 neurons were traced per section. For axons in the CST, 1 section was analyzed per mouse and approximately 10 neurons were traced per sections.

Statistical analysis. All statistical analyses were performed using the Prism software (version 6; Graphpad Software Inc., La Jolla, CA, USA). Statistical differences were determined by D'Agostinos and Pearson normality test and two-tailed unpaired *t*-test, Mann–Whitney test or one-way ANOVA followed by *post hoc* Tukey's multiple comparison test. Statistically significant differences were considered at $P<0.05$, and values were expressed as the independent mean ± s.e.m. *P* or adjusted *P*-values are presented when statistically significant differences are reported.

CONFLICT OF INTEREST

The authors declare no conflict of interest.

ACKNOWLEDGEMENTS

This work was supported by grants from Les Turner ALS and Wenske Foundations (to PHO), NUCATS (to PHO and MCB), 1R01NS085161-01 (to PHO), ALSA Safenowitz fellowship (to JHJ) and Northwestern Weinberg Grant (to MJS). WD Weber and J Xie helped with histochemistry. Stephanie R Villa contributed to the generation of

preliminary findings. We also thank the Microscopy and Imaging Facility at Stanley Manne Children's Research Institute and B Goossens for help with confocal microscopy.

REFERENCES

1 Jones EG, Schreyer DJ, Wise SP. Growth and maturation of the rat corticospinal tract. *Prog Brain Res* 1982; **57**: 361–379.
2 Lemon RN. Descending pathways in motor control. *Annu Rev Neurosci* 2008; **31**: 195–218.
3 Jara JH, Genc B, Klessner JL, Ozdinler PH. Retrograde labeling, transduction, and genetic targeting allow cellular analysis of corticospinal motor neurons: implications in health and disease. *Front Neuroanat* 2014; **8**: 16.
4 Alstermark B, Isa T. Circuits for skilled reaching and grasping. *Annu Rev Neurosci* 2012; **35**: 559–578.
5 Heckman CJ, Enoka RM. Motor unit. *Compr Physiol* 2012; **2**: 2629–2682.
6 Shepherd GM. The microcircuit concept applied to cortical evolution: from three-layer to six-layer cortex. *Front Neuroanat* 2011; **5**: 30.
7 Fogarty MJ, Noakes PG, Bellingham MC. Motor cortex layer V pyramidal neurons exhibit dendritic regression, spine loss, and increased synaptic excitation in the presymptomatic hSOD1G93A mouse model of amyotrophic lateral sclerosis. *J Neurosci* 2015; **35**: 643–647.
8 Molyneaux BJ, Arlotta P, Menezes JR, Macklis JD. Neuronal subtype specification in the cerebral cortex. *Nat Rev Neurosci* 2007; **8**: 427–437.
9 Fink JK. Hereditary spastic paraplegia: clinico-pathologic features and emerging molecular mechanisms. *Acta Neuropathol* 2013; **126**: 307–328.
10 Robberecht W, Philips T. The changing scene of amyotrophic lateral sclerosis. *Nat Rev Neurosci* 2013; **14**: 248–264.
11 Novarino G, Fenstermaker AG, Zaki MS, Hofree M, Silhavy JL, Heiberg AD *et al.* Exome sequencing links corticospinal motor neuron disease to common neurodegenerative disorders. *Science* 2014; **343**: 506–511.
12 Feringa ER, Gilbertie WJ, Vahlsing HL. Histologic evidence for death of cortical neurons after spinal cord transection. *Neurology* 1984; **34**: 1002–1006.
13 Hains BC, Black JA, Waxman SG. Primary cortical motor neurons undergo apoptosis after axotomizing spinal cord injury. *J Comp Neurol* 2003; **462**: 328–341.
14 Dugas JC, Mandemakers W, Rogers M, Ibrahim A, Daneman R, Barres BA. A novel purification method for CNS projection neurons leads to the identification of brain vascular cells as a source of trophic support for corticospinal motor neurons. *J Neurosci* 2008; **28**: 8294–8305.
15 Jara JH, Villa SR, Khan NA, Bohn MC, Ozdinler PH. AAV2 mediated retrograde transduction of corticospinal motor neurons reveals initial and selective apical dendrite degeneration in ALS. *Neurobiol Dis* 2012; **47**: 174–183.
16 Yasvoina MV, Genc B, Jara JH, Sheets PL, Quinlan KA, Milosevic A *et al.* eGFP expression under UCHL1 promoter genetically labels corticospinal motor neurons and a subpopulation of degeneration-resistant spinal motor neurons in an ALS mouse model. *J Neurosci* 2013; **33**: 7890–7904.
17 Davidson BL, Bohn MC. Recombinant adenovirus: a gene transfer vector for study and treatment of CNS diseases. *Exp Neurol* 1997; **144**: 125–130.
18 Daya S, Berns KI. Gene therapy using adeno-associated virus vectors. *Clin Microbiol Rev* 2008; **21**: 583–593.
19 LeWitt PA, Rezai AR, Leehey MA, Ojemann SG, Flaherty AW, Eskandar EN *et al.* AAV2-GAD gene therapy for advanced Parkinson's disease: a double-blind, sham-surgery controlled, randomised trial. *Lancet Neurol* 2011; **10**: 309–319.
20 McCown TJ. Adeno-associated virus (AAV) vectors in the CNS. *Curr Gene Ther* 2005; **5**: 333–338.
21 Burger C, Nash K, Mandel RJ. Recombinant adeno-associated viral vectors in the nervous system. *Hum Gene Ther* 2005; **16**: 781–791.
22 Hutson TH, Verhaagen J, Yanez-Munoz RJ, Moon LD. Corticospinal tract transduction: a comparison of seven adeno-associated viral vector serotypes and a non-integrating lentiviral vector. *Gene Therapy* 2012; **19**: 49–60.
23 Blits B, Derks S, Twisk J, Ehlert E, Prins J, Verhaagen J. Adeno-associated viral vector (AAV)-mediated gene transfer in the red nucleus of the adult rat brain: comparative analysis of the transduction properties of seven AAV serotypes and lentiviral vectors. *J Neurosci Methods* 2010; **185**: 257–263.
24 Paxinos G, Franklin KBJ. *The Mouse Brain in Stereotaxic Coordinates*, 2nd edn. Academic Press: San Diego, CA, USA, 2001.
25 Klein RL, Dayton RD, Tatom JB, Henderson KM, Henning PP. AAV8, 9, Rh10, Rh43 vector gene transfer in the rat brain: effects of serotype, promoter and purification method. *Mol Ther* 2008; **16**: 89–96.
26 Passini MA, Watson DJ, Wolfe JH. Gene delivery to the mouse brain with adeno-associated virus. *Methods Mol Biol* 2004; **246**: 225–236.
27 Petrs-Silva H, Dinculescu A, Li Q, Deng WT, Pang JJ, Min SH *et al.* Novel properties of tyrosine-mutant AAV2 vectors in the mouse retina. *Mol Ther* 2011; **19**: 293–301.
28 Longair MH, Baker DA, Armstrong JD. Simple Neurite Tracer: open source software for reconstruction, visualization and analysis of neuronal processes. *Bioinformatics* 2011; **27**: 2453–2454.
29 Ozdinler PH, Benn S, Yamamoto TH, Guzel M, Brown Jr RH, Macklis JD. Corticospinal motor neurons and related subcerebral projection neurons undergo early and specific neurodegeneration in hSOD1G93A transgenic ALS mice. *J Neurosci* 2011; **31**: 4166–4177.
30 Thomsen GM, Gowing G, Latter J, Chen M, Vit JP, Staggenborg K *et al.* Delayed disease onset and extended survival in the SOD1G93A rat model of amyotrophic lateral sclerosis after suppression of mutant SOD1 in the motor cortex. *J Neurosci* 2014; **34**: 15587–15600.
31 Henriques A, Pitzer C, Dittgen T, Klugmann M, Dupuis L, Schneider A. CNS-targeted viral delivery of G-CSF in an animal model for ALS: improved efficacy and preservation of the neuromuscular unit. *Mol Ther* 2011; **19**: 284–292.
32 Martinov VN, Sefland I, Walaas SI, Lomo T, Nja A, Hoover F. Targeting functional subtypes of spinal motoneurons and skeletal muscle fibers in vivo by intramuscular injection of adenoviral and adeno-associated viral vectors. *Anat Embryol* 2002; **205**: 215–221.
33 Towne C, Setola V, Schneider BL, Aebischer P. Neuroprotection by gene therapy targeting mutant SOD1 in individual pools of motor neurons does not translate into therapeutic benefit in fALS mice. *Mol Ther* 2011; **19**: 274–283.
34 Kaspar BK, Llado J, Sherkat N, Rothstein JD, Gage FH. Retrograde viral delivery of IGF-1 prolongs survival in a mouse ALS model. *Science* 2003; **301**: 839–842.
35 Dodge JC, Treleaven CM, Fidler JA, Hester M, Haidet A, Handy C *et al.* AAV4-mediated expression of IGF-1 and VEGF within cellular components of the ventricular system improves survival outcome in familial ALS mice. *Mol Ther* 2010; **18**: 2075–2084.
36 Towne C, Raoul C, Schneider BL, Aebischer P. Systemic AAV6 delivery mediating RNA interference against SOD1: neuromuscular transduction does not alter disease progression in fALS mice. *Mol Ther* 2008; **16**: 1018–1025.
37 Foust KD, Nurre E, Montgomery CL, Hernandez A, Chan CM, Kaspar BK. Intravascular AAV9 preferentially targets neonatal neurons and adult astrocytes. *Nat Biotechnol* 2009; **27**: 59–65.
38 Foust KD, Salazar DL, Likhite S, Ferraiuolo L, Ditsworth D, Ilieva H *et al.* Therapeutic AAV9-mediated suppression of mutant SOD1 slows disease progression and extends survival in models of inherited ALS. *Mol Ther* 2013; **21**: 2148–2159.
39 Foust KD, Poirier A, Pacak CA, Mandel RJ, Flotte TR. Neonatal intraperitoneal or intravenous injections of recombinant adeno-associated virus type 8 transduce dorsal root ganglia and lower motor neurons. *Hum Gene Ther.* 2008; **19**: 61–70.
40 Cearley CN, Wolfe JH. Transduction characteristics of adeno-associated virus vectors expressing cap serotypes 7, 8, 9, and Rh10 in the mouse brain. *Mol Ther* 2006; **13**: 528–537.
41 Taymans JM, Vandenberghe LH, Haute CV, Thiry I, Deroose CM, Mortelmans L *et al.* Comparative analysis of adeno-associated viral vector serotypes 1, 2, 5, 7, and 8 in mouse brain. *Hum Gene Ther* 2007; **18**: 195–206.
42 Broekman ML, Comer LA, Hyman BT, Sena-Esteves M. Adeno-associated virus vectors serotyped with AAV8 capsid are more efficient than AAV-1 or -2 serotypes for widespread gene delivery to the neonatal mouse brain. *Neuroscience* 2006; **138**: 501–510.
43 Burger C, Gorbatyuk OS, Velardo MJ, Peden CS, Williams P, Zolotukhin S *et al.* Recombinant AAV viral vectors pseudotyped with viral capsids from serotypes 1, 2, and 5 display differential efficiency and cell tropism after delivery to different regions of the central nervous system. *Mol Ther* 2004; **10**: 302–317.
44 Davidson BL, Stein CS, Heth JA, Martins I, Kotin RM, Derksen TA *et al.* Recombinant adeno-associated virus type 2, 4, and 5 vectors: transduction of variant cell types and regions in the mammalian central nervous system. *Proc Natl Acad Sci USA* 2000; **97**: 3428–3432.
45 Aschauer DF, Kreuz S, Rumpel S. Analysis of transduction efficiency, tropism and axonal transport of AAV serotypes 1, 2, 5, 6, 8 and 9 in the mouse brain. *PLoS One* 2013; **8**: e76310.
46 Nathanson JL, Yanagawa Y, Obata K, Callaway EM. Preferential labeling of inhibitory and excitatory cortical neurons by endogenous tropism of adeno-associated virus and lentivirus vectors. *Neuroscience* 2009; **161**: 441–450.
47 Manfredi A, Marrocco E, Puppo A, Cesi G, Sommella A, Della Corte M *et al.* Combined rod and cone transduction by adeno-associated virus 2/8. *Hum Gene Ther* 2013; **24**: 982–992.
48 Chen BD, He CH, Chen XC, Pan S, Liu F, Ma X *et al.* Targeting transgene to the heart and liver with AAV9 by different promoters. *Clin Exp Pharmacol Physiol* 2015; **42**: 1108–1117.
49 King AE, Blizzard CA, Southam KA, Vickers JC, Dickson TC. Degeneration of axons in spinal white matter in G93A mSOD1 mouse characterized by NFL and alpha-internexin immunoreactivity. *Brain Res* 2012; **1465**: 90–100.
50 Ohno T, Maeda H, Sakurai M. Regionally specific distribution of corticospinal synapses because of activity-dependent synapse elimination in vitro. *J Neurosci* 2004; **24**: 1377–1384.
51 Takuma H, Sakurai M, Kanazawa I. In vitro formation of corticospinal synapses in an organotypic slice co-culture. *Neuroscience* 2002; **109**: 359–370.

52 Yoshioka N, Murabe N, Sakurai M. Regressive events in rat corticospinal axons during development in in vitro slice cocultures: retraction, amputation, and degeneration. *J Comp Neurol* 2009; **513**: 164–172.
53 Asante CO, Martin JH. Differential joint-specific corticospinal tract projections within the cervical enlargement. *PLoS One* 2013; **8**: e74454.
54 Bareyre FM, Kerschensteiner M, Misgeld T, Sanes JR. Transgenic labeling of the corticospinal tract for monitoring axonal responses to spinal cord injury. *Nat Med* 2005; **11**: 1355–1360.
55 Gurney ME, Pu H, Chiu AY, Dal Canto MC, Polchow CY, Alexander DD *et al*. Motor neuron degeneration in mice that express a human Cu,Zn superoxide dismutase mutation. *Science* 1994; **264**: 1772–1775.
56 Lock M, Alvira M, Vandenberghe LH, Samanta A, Toelen J, Debyser Z *et al*. Rapid, simple, and versatile manufacturing of recombinant adeno-associated viral vectors at scale. *Hum Gene Ther* 2010; **21**: 1259–1271.
57 Burger C, Nguyen FN, Deng J, Mandel RJ. Systemic mannitol-induced hyperosmolality amplifies rAAV2-mediated striatal transduction to a greater extent than local co-infusion. *Mol Ther* 2005; **11**: 327–331.
58 Niwa H, Yamamura K, Miyazaki J. Efficient selection for high-expression transfectants with a novel eukaryotic vector. *Gene* 1991; **108**: 193–199.
59 Zhong L, Li B, Mah CS, Govindasamy L, Agbandje-McKenna M, Cooper M *et al*. Next generation of adeno-associated virus 2 vectors: point mutations in tyrosines lead to high-efficiency transduction at lower doses. *Proc Natl Acad Sci USA* 2008; **105**: 7827–7832.
60 Schindelin J, Arganda-Carreras I, Frise E, Kaynig V, Longair M, Pietzsch T *et al*. Fiji: an open-source platform for biological-image analysis. *Nat Methods* 2012; **9**: 676–682.

Supplementary Information accompanies this paper on Gene Therapy website (http://www.nature.com/gt)